Journal of Heat and Mass Transfer Research

Journal homepage: https://jhmtr.semnan.ac.ir

Semnan University

ISSN: 2383-3068

Research Article

Improvement of Energy, Exergy Efficiency and PEC Index in a Heat Exchanger Equipped with Turbulators under the Effect of a Magnetic Field

Alireza Aghaei *, Alireza Mirzaei, Abolfazl Fattahi

Faculty of Mechanical Engineering, University of Kashan, Kashan, Iran

ARTICLE INFO

Article history:

Received: 2025-01-04

Revised: 2025-04-05

Accepted: 2025-07-21

Keywords:

Double-tube heat exchanger;
Vortex generator;
Two-phase flow;
Magnetic field, hybrid nanofluid;
Exergy efficiency.

ABSTRACT

A double-tube heat exchanger equipped with vortex generators is simulated under the influence of a magnetic field. The internal tube of this heat exchanger is equipped with blade-type vortex generators with various geometrical shapes. A magnetic field is employed to enhance thermal efficiency in the double-tube heat exchanger, with Hartmann numbers ranging from 35 to 155. The applied hybrid nanofluid is composed of Syltherm 800, iron oxide, and graphene oxide at volume fractions (φ) of 0, 1.75, and 3.75%. The study is conducted under steady-state conditions using a two-phase model with Reynolds number ranging from 25,000 to 55,000, utilizing the k-epsilon turbulence model. The results indicate that as the Re increases, the convective heat transfer coefficient rises. The maximum increase in the Nusselt number is observed in the heat exchanger equipped with vortex generators of Sample 3, whereas the minimum value occurs in the bare heat exchanger. Additionally, as the Hartmann number increases from 35 to 155, the exergy efficiency also rises. Exergy efficiency increases with Reynolds number up to 35,000 and then decreases. It is also found that the application of a magnetic field maximizes the exergy efficiency at a Re of 35,000 and Hartmann number of 155 for the heat exchanger equipped with Sample 3 vortex generators.

1. Introduction

The double-tube heat exchanger is categorized based on flow type into counterflow and parallel flow. Counterflow double-tube heat exchangers are applicable in scenarios where the fluid flow rate is low or where there is a significant temperature or pressure difference between the two fluids. Researchers have extensively utilized passive methods to enhance thermal performance and optimize exergy efficiency in these types of exchangers. Bayat and Nikseresht [1] studied the effect of water-aluminum oxide nanofluid on flow fields and heat transfer within a duct. Their study was conducted for Reynolds number (Re) ranging from 5,000 to 20,000 and volume fractions of nanoparticles of 1 to 10%. For turbulent flow modeling, they employed the k-epsilon turbulence model. The maximum heat transfer enhancement occurs at a Re of 20,000 and a φ of 10 percent, amounting to a 19.76% increase. Bouya [2] studied the use of twisted turbulators on the hydraulic-thermal performance within a heat exchanger. The primary objective of their study was to compare the increase in heat transfer rate and pressure drop when using one

* **Corresponding author.**
E-mail address: a.aghaei@kashanu.ac.ir

Cite this article as:
Aghaei, A., Mirzaei, A. and Fattahi, A., 2026. Improvement of Energy, Exergy Efficiency and PEC Index in a Heat Exchanger Equipped with Turbulators under the Effect of a Magnetic Field. *Journal of Heat and Mass Transfer Research*, 13(2), pp. 193-206.
https://doi.org/10.22075/JHMTR.2025.36432.1672

to three twisted turbulators. Their study was conducted in a turbulent flow regime with Res ranging from 6,000 to 36,000. The output results were presented as Nu curves, pressure drop, and friction coefficient. The results indicated that as the number of turbulators increased, both heat transfer and pressure drop increased. Furthermore, an increase in velocity correlated directly with improved thermal performance. Waghol et al. [3] conducted an experimental study on the impact of twisted turbulators on the hydraulic and thermal performance of a water-silver nanofluid in a solar collector. Their study examined φ of 1% to 5% of silver nanoparticles and Res ranging from 4000 to 16000 in a turbulent flow regime. Their results indicated that the water-silver nanofluid performed thermally better than the base fluid (water), with a 21.64% increase in Nu. Pressure drop showed a direct relationship with both the Re and the φ of nanoparticles. Eiamsa-ard et al. [4] investigated the effect of using helical strips in heat exchangers filled with water-copper oxide nanofluid. Their study was conducted over a Re range of 8000 to 36000. They used the k-epsilon turbulence model for simulating turbulent flow, and the nanofluid was modeled as a single phase. The results showed that increasing the pitch of the helical strips enhanced heat transfer and pressure drop at the outlet of the heat exchanger. Kim [5] performed a study on the flow field and heat transfer within a twisted tube at various pitch ratios in a turbulent flow regime. According to their findings, increasing the pitch in the fluid-carrying tube generated vortices, which enhanced heat transfer. Ahmad et al. [6] investigated the effect of angled turbulators on the hydraulic and thermal performance of nanofluid within a channel. They utilized a nanofluid composed of silicon oxide and aluminum oxide particles. The study was conducted in a turbulent flow regime with Res ranging from 8000 to 32000. Their results indicated that the simultaneous use of turbulators and nanofluids could improve thermal performance by up to 67.93%. Furthermore, employing turbulators and nanofluids at high nanoparticle volume fractions (high φ) increased the pressure drop. Zhang et al. [7] investigated the thermal behavior of a nanofluid in a microchannel. According to their results, the Nu in the microchannel increases with the increase in the φ of nanoparticles. Moshofi et al. [8] conducted an experimental study on the effects of helical strips on the flow field and heat transfer within a duct. Their study was performed in a turbulent flow regime with Res ranging from 7000 to 35000. The authors presented their results as curves of Nus, pressure drop, and friction coefficients. According to their findings, the use of helical strips at high Res created significantly more mixing and turbulence than at lower Res, which, as expected, resulted in higher heat transfer rates. Sheikholeslami et al. [9] investigated the effect of perforated turbulators on the flow field and heat transfer within a double-pipe heat exchanger. The main goal of their study was to enhance the thermal efficiency of the double-pipe heat exchanger using perforated turbulators. According to their reports, the use of perforated turbulators resulted in a significant pressure drop within the double-pipe heat exchanger, while the heat transfer was positively affected by the presence of the perforated turbulator. Shirvan et al. [10] numerically examined the effect of nanoparticle φ and variable inlet velocity in a double-pipe heat exchanger. The authors investigated the flow regime assuming laminar conditions with Res ranging from 50 to 250. Panahee and Zamzamian [11] conducted an experimental study on the effect of spring-type turbulators with varying pitches on the thermal hydraulic performance within a heat exchanger. Their study examined pitches of 0.5, 1, 1.5, and 2, and a Re range of 10,000 to 50,000 in turbulent flow. According to their results, as the inlet velocity and the pitch of the spring turbulators increased, the convective heat transfer coefficient, as a representative of heat transfer in the thermal system, also increased. Bazarpour and Goharkhah [12] used numerical methods to investigate the double-tube heat exchanger under various concentrations. The results indicated that using an external magnetic field could increase heat transfer by up to 320%, and due to the absence of additional obstacles in the flow path, resistance to flow and thus pressure drop is minimized. The heat transfer coefficient had a direct relationship with both the Re and concentration, increasing for both hot and cold flows under the magnetic field. Sheikholeslami [13] investigated the heat transfer rate of a nanofluid in an enclosure with V-shape fins. They reported an improvement in the Nu for both fluid types. Kang Chi et al. [14] studied the convective heat transfer of iron oxide-water nanofluid in a rectangular cavity under a magnetic field. Factors such as nanoparticle concentration, horizontal and vertical magnetic field orientations, magnetic field intensity, and cavity rotation angle were considered. The results revealed that as the nanoparticle concentration increased, Nu initially increased and then decreased, reaching a maximum at a concentration of 0.3%. Abdulrazak et al. [15] employed both numerical and experimental methods to analyze heat transfer and the

hydrodynamic behavior of flow through a single-tube heat exchanger with circular and square cross-sections, assessing the performance of two nanofluids with metal oxide and aluminum oxide compared to distilled water under uniform heat flux. Their results demonstrated that non-covalent graphene, due to its higher viscosity and lower thermal performance, was unsuitable for general heat transfer. Moreover, distilled water exhibited the highest performance index among all tested fluids. Barbrowich and Biki´c [16] used numerical methods to investigate heat transfer in laminar flow of silicon nitride nanofluid based on ethylene glycol, modeled as a single-phase mixture in a straight horizontal tube. The tube was subjected to forced convective heat transfer with a constant heat flux. The results indicated that the heat transfer coefficient increased with higher nanoparticle concentrations and flow rates. Behiraei et al. [17] used numerical methods to explore the application of a graphene-based biological nanofluid and the use of two coaxially twisted strips to enhance heat transfer within tubes. The results indicated that using twisted strips with a low twist ratio and nanofluid instead of pure fluid increased heat transfer. Hajialigol and Daghigh [18] studied the effect of using nanofluids and magnetic fields. They employed an ANN approach to predict the behavior of hybrid nanofluid flow. The findings show that using a hybrid nanofluid provided better thermal performance than the base fluid, and the magnetic field enhanced thermal performance. Zhou et al. [19] numerically investigated the effect of a constant magnetic field at various Hartmann numbers on the hydrodynamic behavior of hybrid nanofluid flow in a heat exchanger with rectangular fins. The study was conducted in turbulent flow, considering a two-phase model for simulating hybrid nanofluids. Their results indicated that applying magnetic force at high Res had a greater impact on the flow field and heat transfer. Baskhar et al. [20] examined the effect of a rotating magnetic field in a channel containing magnetic nanofluid. This study was conducted under transitional conditions with high inlet velocities. The results show that the magnetic field induces rotation in the magnetic nanofluid flow. In other words, magnetic nanoparticles were influenced by the magnetic field, causing the flow to become rotational. Based on the reviewed studies, there has been no research on the shape of vortex generators in a double-pipe heat exchanger under the influence of a magnetic field. Therefore, in this study, the geometry of vortex generators is modeled in various configurations, and their impact on hydraulic-thermal performance and exergy efficiency is examined. A magnetic field is utilized with the aim of enhancing thermal efficiency in the double-pipe heat exchanger. Tavakoli et al. [21] at this study numerically investigates the performance of a parabolic trough solar collector (PTC) equipped with a hybrid nanofluid of water/alumina-multiwalled carbon nanotubes (Al_2O_3−MWCNT), analyzing the impact of installing twisted perforated and bladed turbulators on three main indicators: "entropy generation," "collector efficiency," and "performance evaluation criterion (PEC)." In this research, the Eulerian-Eulerian two-phase model, the k-ω turbulence model, the finite volume method (FVM), and the SIMPLEC algorithm are used for the numerical simulation of the flow in the Reynolds number range of 5000 to 35000 and nanoparticle volume fraction of 0 to 3%. The results show that changing the turbulator type from perforated to bladed under optimal conditions (Re=30,000 and φ=3%) leads to a 40.07% reduction in total entropy generation. Furthermore, the highest changes in collector efficiency (1.62%) and normalized entropy number (13.65%) are observed at Re=20,000 (φ=0%) and Re=15,000 (φ=1%), respectively. Based on the performed analyses, the twisted perforated turbulator was identified as the more desirable option for use in this system due to improved heat transfer, reduced entropy generation, and increased collector efficiency. El-Shafay et al. [22] investigated the simultaneous effect of Cu-ZnO/water hybrid nanofluid and helical twisted tape (HTT) turbulator on the exergy efficiency and thermohydraulic performance of a heat exchanger, using the finite volume method (FVM) and solidworks software for geometry modeling. The simulations were performed under steady-state flow conditions, employing a pressure-based solver, and the hybrid nanofluid behavior was analyzed based on the mixture model. The main parameters considered were Reynolds number (10,000 to 40,000), nanoparticle volume fraction (1 to 5%), and twist ratio (1 to 4). The results indicate that increasing the Reynolds number and nanoparticle volume fraction significantly improves the average Nusselt number (Nu_{av}) and the thermal performance of the exchanger. Specifically, at φ = 5% and Re = 40,000, the use of the HTT turbulator with a twist ratio of 4 results in a 180.97% increase in pressure drop compared to the case without a turbulator. On the other hand, under the same conditions, increasing the Reynolds number from 10,000 to 40,000 leads to a 38.89% increase in exergy efficiency, with the highest exergy efficiency achieved in the presence of a magnetic field with a Hartmann number of 150 and Re = 20,000. Mohadjer et al. [23] numerically analyzed the

potential negative effects of twisted tapes on the average Nusselt number (Nu), friction factor (f), flow behavior, and Performance Evaluation Criteria (PEC) in a water-titania nanofluid using a three-dimensional method. The study examined 156 different cases, encompassing diverse turbulator designs (with varying number of blades and twist ratios). The results indicate that only 25%, 25%, and 22.9% of the investigated cases at Reynolds numbers of 4000, 6000, and 8000, respectively, lead to a PEC greater than 1. Although turbulators can increase the Nusselt number by up to 65.1% in the best-case scenario, they also increase the friction factor by more than 6 times. Furthermore, in some configurations (such as a three-bladed turbulator with a pitch ratio of 11), the PEC decreased by up to 11.8%, which is more severe than the maximum improvement (6.3%). Analysis of the velocity field and streamlines also reveals the unfavorable impact of these devices on the flow pattern. These findings suggest that incorrect selection of the turbulator design not only fails to create a significant improvement in performance but may also lead to a decrease in system efficiency. Therefore, the application of these methods requires careful consideration of design parameters and a balance between increased heat transfer and hydraulic losses. Wang et al. [24] numerically investigated the performance of a heat exchanger equipped with a perforated conical turbulator and water/Fe_2O_3 nanofluid. The main innovation of this research lies in designing a passive method to enhance heat transfer through the integration of a modified conical turbulator and nanofluid, an approach that has received less attention in the existing literature. Using advanced computational fluid dynamics (CFD) modeling, the influence of various parameters, including Reynolds number (4000 to 20,000), nanoparticle percentage (up to 2%), and turbulator geometry, on the thermo-hydraulic performance of the system was analyzed. Key findings show that this novel turbulator increases the Nusselt number by 3.4 to 5.4 times and the friction factor by 1.8 to 2.3 times compared to smooth tubes. Specifically, adding only 2% Fe_2O_3 nanoparticles results in a 92% increase in the Nusselt number.

2. Geometrical Model and Governing Equations

The three-dimensional geometry model of the double-pipe heat exchanger equipped with vortex generators under the effect of a magnetic field is presented in figure 1.

As can be seen, the inner tube of this heat exchanger is equipped with blade-type vortex generators in three shapes called Sample 1 to 3. The geometry of the vortex generators has been modeled in various geometric configurations, and their impact on hydraulic-thermal performance and exergy efficiency is examined. A magnetic field is utilized in this study to enhance thermal efficiency in the double-pipe heat exchanger. The magnetic field is analyzed at Hartmann numbers ranging from 35 to 155. The hybrid nanofluid Syltherm 800-iron oxide-graphene is used as the working fluid at φ of 0%, 1.75%, and 3.75%. The study is conducted in a steady state and in a turbulent flow regime within the Re range of 25,000 to 55,000, using the k-epsilon turbulence model. Additionally, the SIMPLEC algorithm will be used to couple the velocity and pressure equations. As shown in figure 1, a portion of the inner tube is equipped with three types vortex generator and is under the effect of a magnetic field.

The current study focuses on integrating various technologies (magnetic field, hybrid nanofluid, and novel turbulence-generating geometries) and providing a comprehensive analysis of their interaction on key metrics (energy, exergy, and PEC). This approach offers a new framework for designing high-efficiency heat exchangers in energy industries. Sheikholeslami et al. [25] have taken an effective step towards improving the performance of CPVT (Concentrated Photovoltaic/Thermal) systems by introducing a novel configuration based on the integration of a parabolic trough concentrator, a heat sink, and a vortex generator (VG). In this research, the effect of various parameters, including the VG angle (θ = 30° and 60°), pitch ratio (S = 0.025 to 0.05), and volumetric flow rate (Q = 0.5 to 2 liters per minute) on the thermal and electrical performance of the system was investigated using numerical simulations and radiation modeling. The results show that installing the VG changes the water flow regime from laminar to turbulent, and the highest thermal efficiency (63.75%) and electrical efficiency (13.96%) are obtained under optimal conditions (θ = 30°, S = 0.025, and Q = 2 liters per minute). Adding the VG alone results in a 1.42% improvement in thermal efficiency and a 2.74% improvement in electrical efficiency, while increasing the angle and pitch ratio of the VG has a reverse effect on the system's performance. On the other hand, increasing the flow rate up to 2 liters per minute leads to a 1.17% increase in thermal efficiency and a 2.55% increase in electrical efficiency for the optimal case.

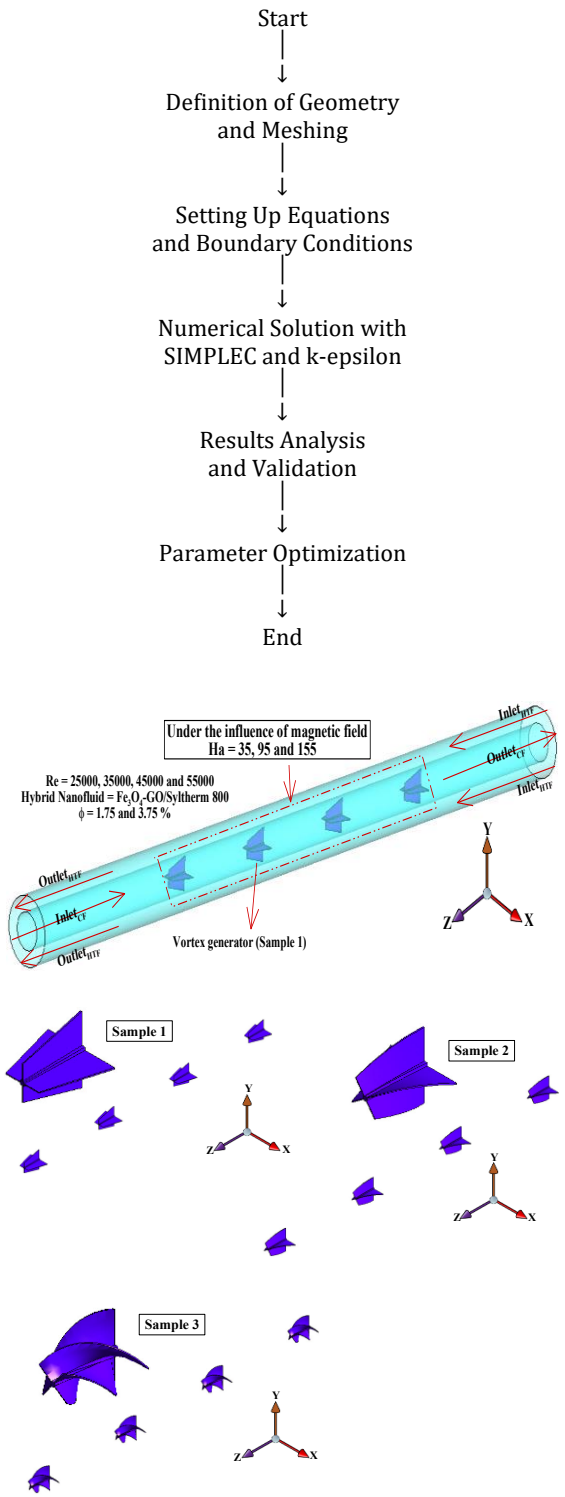

Fig. 1. Schematic geometry of the double-tube heat exchanger

As shown in figure 1, a portion of the inner tube is equipped with a vortex generator and is under the effect of a magnetic field. For modeling the hybrid nanofluid, a two-phase model is used. The governing equations for the three-dimensional geometry of the double-tube heat exchanger are written as Equations 1 to 16. Equations 1, 2, and 4 correspond to the continuity, momentum, and energy equations, respectively. Equation 3 represents the φ relationship, where ϕ is the φ of phase k. Since the magnetic field is considered in this problem, Equation 5 pertains to the density flux. Additionally, the electric potential is calculated using Equation 6. The density, specific heat capacity, thermal conductivity of the mixture, and viscosity in the mixture model can be determined using Equations 7 to 10. In these equations, $\vec{V}_{dr.bf}$ is the drift velocity of the nanoparticles and $\vec{V}_{dr.s}$ is the drift velocity of the base fluid water [26-28].

$$\nabla.(\rho_m V_m) = 0 \tag{1}$$

$$\nabla.(\rho_m \vec{V}_m \vec{V}_m) = -\nabla p + \nabla.\left[\mu_m(\nabla\vec{V}_m + \nabla\vec{V}_m^T) + \left(\sum_{k=1}^{n} \phi_k \rho_k \vec{V}_{dr,k}\vec{V}_{dr,k}\right)\right] + [\vec{J}\times\vec{B}] \tag{2}$$

$$\nabla.\left(\phi_p \rho_p \vec{V}_m\right) = -\nabla(\phi_p \rho_p \vec{V}_{dr,p}) \tag{3}$$

$$\nabla.\left[\phi_k V_k\left(\phi_p h_k + p\right)\right] = \nabla.\left(k_{eff}\nabla T - C_{p,m}\rho_m \vec{V}t\right) + \frac{J^2}{\sigma_m} \tag{4}$$

$$\vec{\nabla}.\vec{J} = 0 \tag{5}$$

$$\vec{\nabla}.(\vec{\nabla}\zeta) = \vec{\nabla}.(\vec{V}_m \times \vec{B}) \tag{6}$$

$$\rho_m = \sum_{k=1}^{n} \phi_k \rho_k \tag{7}$$

$$C_{p,m} = \frac{(1-\phi)\rho_f C_f + \phi\rho_f C_{p,p}}{\rho_m} \tag{8}$$

$$k_{eff} = \sum_{k=1}^{n} \phi_k K_k \tag{9}$$

$$\mu_m = \sum_{k=1}^{n} \phi_k \mu_k \tag{10}$$

$$\sigma_m = \sum_{k=1}^{n} \phi_k \sigma_k \tag{11}$$

$$V_m = \frac{\sum_{k=1}^{n}(\phi_k \mu_k V_k)}{\rho_m} \quad (12)$$

$$V_{dr,k} = V_{pf} - \sum_{k=1}^{n} \frac{\phi_k \rho_k}{\rho_m} V_{f,k} \quad (13)$$

$$V_{pf} = \frac{\rho_p d_p^2}{18\mu f_{drag}} \frac{\left(\rho_p - \rho_m\right)}{\rho_p}(g - (V_m.\nabla)V_m) = V_p - V_f \quad (14)$$

$$f_{drag} = \begin{cases} 1 + 0.15Re_p^{0.687} & Re \leq 1000 \\ 0.0183Re_p & Re > 1000 \end{cases} \quad (15)$$

$$Re = \frac{\rho_f \left|\vec{V}_p - \vec{V}_f\right| d_p}{\mu_f} \quad (16)$$

The thermophysical properties of the working fluids are presented in Table 1. Additionally, equations (17-20) are used to calculate the thermophysical properties of the hybrid nanofluid [29]. The properties of the base fluid, which is Syltherm 800, are referenced from [30]. In this relations, $\vec{U}_m$is the inlet velocity, d_p is the pipe diameter, ρ_{HNF} is the density of the hybrid nanofluid, and μ_{HNF} is the viscosity. Furthermore, the pressure drop in the double-tube heat exchanger can be calculated using Equation 22. The Nu and the performance evaluation criteria are calculated using Equations 23 and 24, respectively. To calculate exergy efficiency, Equation 25 is used [31].

Table 1. Thermophysical properties of the hybrid nanoparticle [32, 33]

No.	Property	Fe3O4	GO	Syltherm 800
1	$\rho\left(kg.m^{-3}\right)$	5200	1910	926
2	$c_P\left(J.kg^{-1}.K^{-1}\right)$	670	710	1.6206
3	$k\left(W.m^{-1}.K^{-1}\right)$	6	1000	0.1331

$$\rho_{HNF} = \rho_{NP1}\phi_{NP1} + \rho_{NP2}\phi_{NP2} + \rho_f(1 - \phi_{NP1} - \phi_{NP2}) \quad (17)$$

$$(c_p)_{HNF} = (c_p)_{NP1}\phi_{NP1} + (c_p)_{NP2}\phi_{NP2} + (c_p)_f(1 - \phi_{NP1} - \phi_{NP2}) \quad (18)$$

$$\mu_{HNF} = \mu_f(1 - \phi_{NP1} - \phi_{NP2})^{-2.5} \quad (19)$$

$$k_{HNF} = k_f \left(\begin{array}{c} (k_{NP1} + k_{NP2}) + 2k_f - \\ 2\varphi_{NP1}(k_f - k_{NP1}) - \\ 2\varphi_{NP2}(k_f - k_{NP2}) \\ \hline (k_{NP1} + k_{NP2}) + 2k_f + \\ \varphi_{NP1}(k_f - k_{NP1}) + \\ \varphi_{NP2}(k_f - k_{NP2}) \end{array} \right) \quad (20)$$

$$Re_{HNF} = \frac{\vec{U}_m d_p \rho_{HNF}}{\mu_{HNF}} \quad (21)$$

$$\Delta P = P_{av,inlet} - P_{av,outlet} \quad (22)$$

$$Nu = \frac{h_{nf} \cdot D_h}{k_{nf}} \quad (23)$$

$$PEC = \frac{\left(\frac{Nu_{nf}}{Nu_f}\right)}{\left(\frac{f_{nf}}{f_f}\right)^{\frac{1}{3}}} \quad (24)$$

$$\eta_{ex} = \frac{m_c C_{p,c} In\frac{T_c^{out}}{T_c^{in}}}{m_h C_{p,h} In\frac{T_h^{out}}{T_h^{in}} + m_c \frac{\Delta P_c}{\rho_c} \frac{In\frac{T_c^{out}}{T_c^{in}}}{T_c^{out} - T_c^{in}} + m_h \frac{\Delta P_h}{\rho_h} \frac{In\frac{T_h^{out}}{T_h^{in}}}{T_h^{out} - T_h^{in}}} \quad (25)$$

3. Boundary Conditions and Numerical Modeling

The differential terms in the momentum and energy equations are discretized using a second-order scheme. The solution procedure is terminated when the residuals of continuity,

momentum, energy, and turbulence equations reach 10^{-5}. The SIMPLEC algorithm is used.

At the inlet, a velocity inlet boundary condition is used, where the velocity is determined based on the Reynolds number. At the outlet of the duct, a pressure outlet boundary condition is applied. A no-slip condition is enforced on all walls and vortex generators. The values of the Hartmann number are shown in figure 1. The incident radiative heat flux is approximately 1200 $\frac{w}{m^2}$. The heat equation is not solved for the vortex generators.

4. Results and Discussion Funding Statement

4.1. Mesh Independence Test and Verification

To identify an appropriate mesh that ensures independence of results from the number of mesh points, the Nu for the hybrid nanofluid within the double-tube heat exchanger, along with the vortex generator (geometric configuration Sample 3), was considered for various mesh point counts and compared in figure 2. Based on the obtained values of the Nu, it can be concluded that a mesh with 1,693,715 cells is suitable.

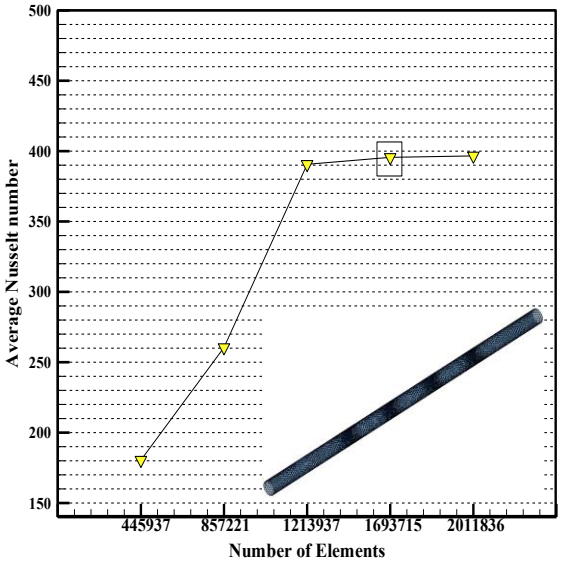

Fig. 2. Mesh independence test for the vortex generator (Sample 3) at φ=3.75% and a Re=55,000.

To ensure the numerical solution's validity, a comparison based on the study of Ma et al. [34] has been conducted. In Ref. [34], the effect of a magnetic field in a two-dimensional channel is numerically investigated. The velocity values obtained in the cross-section of Ref. [34] under the influence of the magnetic field have been compared with the current results in figure 3.

Therefore, the present numerical approach can capture the physics of the problem.

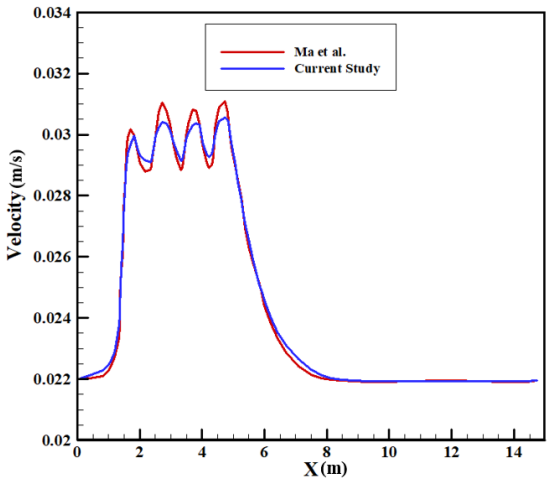

Fig. 3. A comparison between the current results and those derived by Ref. [34]

4.2. Thermal and Hydrodynamic Analysis

The variations of the Nu as a function of the Re in the heat exchanger equipped with a vortex generator with different geometric shapes are shown in figure 4 for various φ. As observed, with the increase in the Re, the heat transfer coefficient also increases, resulting in enhanced heat transfer. As the Re increases, the flow velocity of the hybrid nanofluid increases, thereby raising the Nu. The maximum variation in the Nu occurs in the heat exchanger equipped with the vortex generator in geometric configuration Sample 3, while the minimum variation is observed when the heat exchanger is empty and lacks a vortex generator.

For the base fluid Syltherm 800 at Re=55,000, embedding a Sample 3 vortex generator in the double-tube heat exchanger results in a 58.90% increase in Nu compared to the case without a vortex generator. At a φ of 1.75% and a Re of 55,000, embedding the Sample 3 vortex generator leads to a 59.76% increase in the Nu compared to the condition without the vortex generator. Similarly, at a φ of 3.75% and a Re of 55,000, this type of vortex generator results in a 60.18% increase in the Nu compared to the heat exchanger without the vortex generator.

This improvement can be used in industrial cooling systems such as chemical reactors, power plants, or high-power electronic systems. For example, in an industrial heat exchanger, this increase in Nu (Nusselt number) means reducing equipment size or increasing cooling capacity without needing to change the physical design.

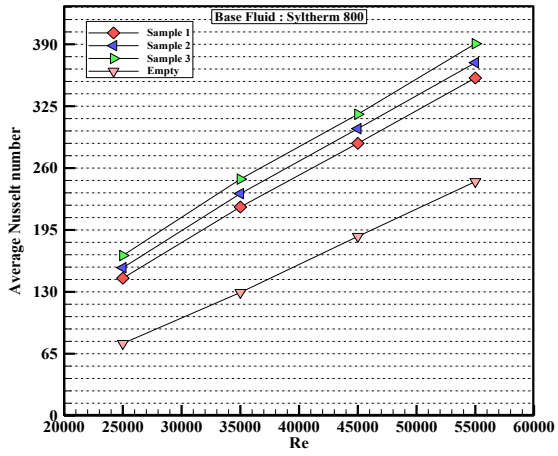

(a)

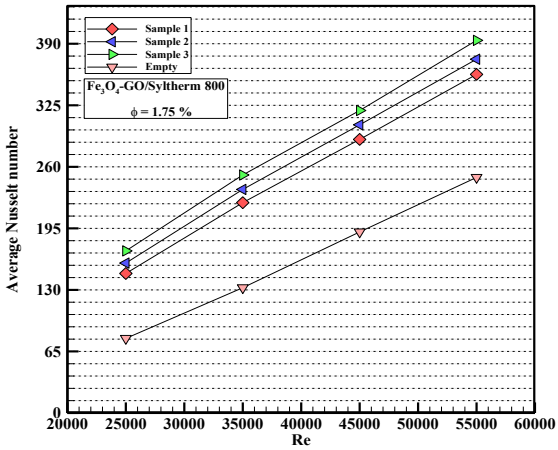

(b)

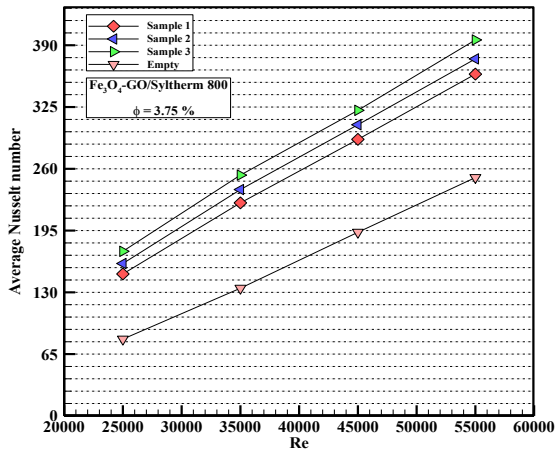

(c)

Fig. 4. Variations of the Nu as a function of the Re in (a) base fluid Syltherm 800, (b) φ of 1.75%, (c) φ of 3.75%.

Figure 5 presents the velocity contours in the heat exchanger equipped with a vortex generator in different geometric configurations. It is evident that the presence of the vortex generator in the flow path can significantly impact the flow behavior. Furthermore, even the slightest geometric changes can alter the behavior of the hybrid nanofluid, leading to significant variations in various parameters.

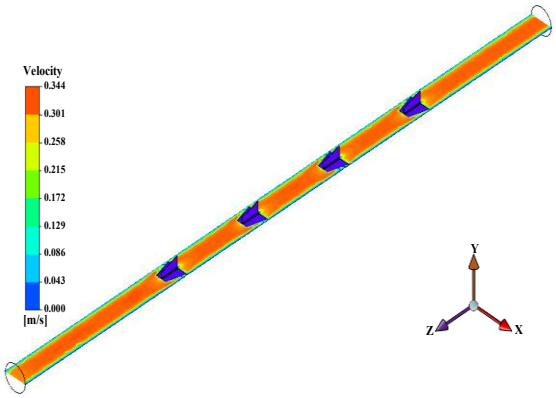

(a)

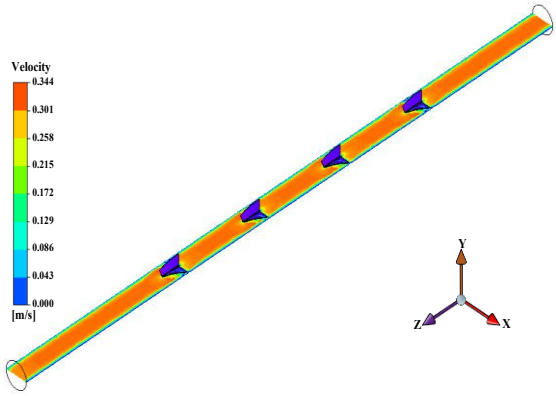

(b)

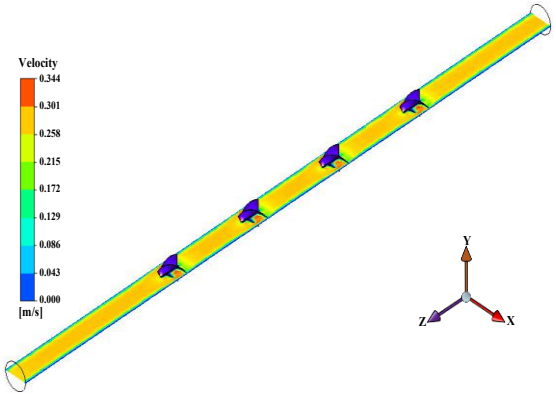

(c)

Fig. 5. Velocity contours for (a) Sample 1, (b) Sample 2 and (c) Sample 3.

Figure 6 illustrates the variation of pressure drop as a function of Re in the heat exchanger equipped with different vortex generators and φ. As observed, with the increase in Re and changes in the geometric shape of the vortex generator in the internal tube of the double-tube heat exchanger, the pressure drop consistently shows an increasing trend in all cases. This is because when the geometric shape of the vortex generator changes, the twist ratio of the blades increases, resulting in a greater contact area between the hybrid nanofluid and the vortex generator, ultimately leading to an increase in pressure drop.

At a Reynolds number of 55,000, the use of the sample 3 vortex generator in the heat exchanger operating with the base fluid Sylthern 800 results in an 84.51% increase in pressure drop compared with the case without a vortex generator. At a nanoparticle volume fraction of φ=1.75% and the same Reynolds number, the pressure drop increases by 85.38% relative to the configuration without the vortex generator. Similarly, at φ=3.75% and Re=55,000, the pressure drop increases by 86.02%.

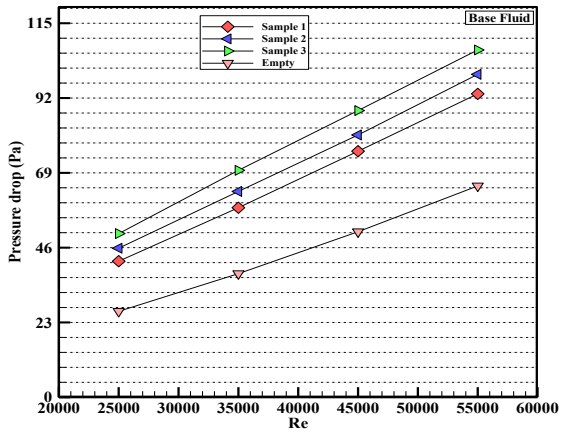

(a)

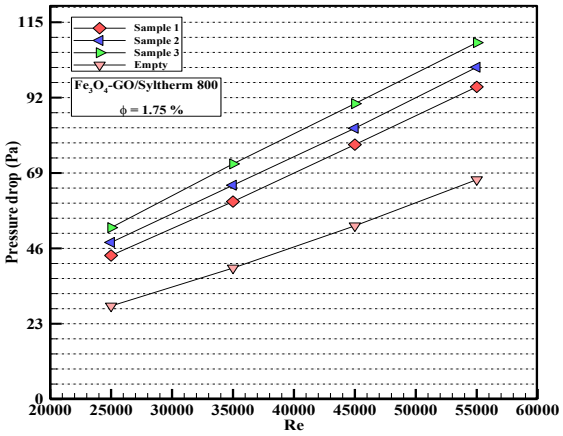

(b)

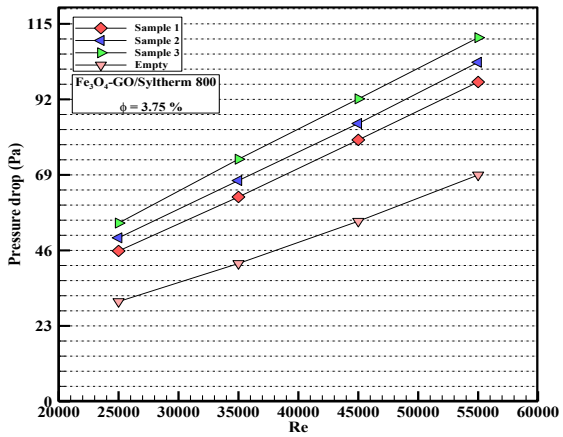

(c)

Fig. 6. Variations of pressure drop as a function of the Re (a) base fluid Sylthern 800, (b) φ of 1.75%, (c) φ of 3.75%.

Figure 7 shows the pressure contours in different geometric configurations. From the obtained results, it can be stated that the maximum variation in pressure occurs by using the Sample 3 vortex generator, while the minimum changes are observed for the bare tubes. The presence of twists in the blades alters the flow lines, enhances mixing, and consequently increases the pressure drop. Therefore, changes in the geometric shape of the vortex generator are directly related to increases in pressure drop values.

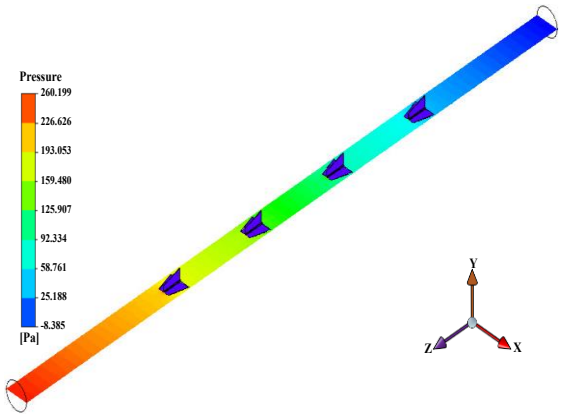

(a)

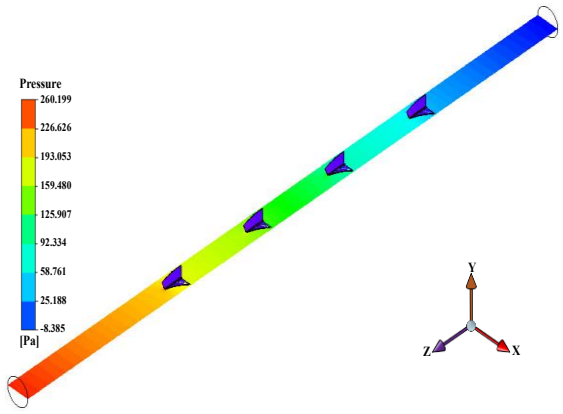

(b)

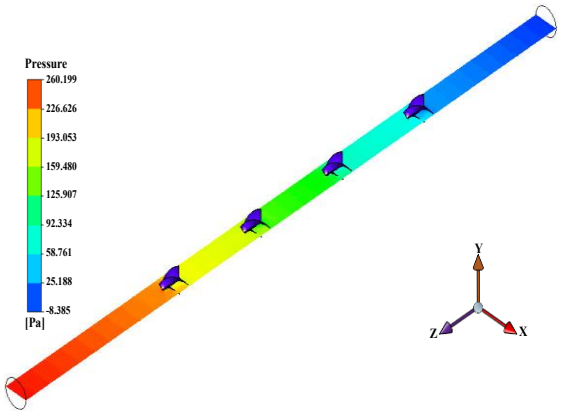

(c)

Fig. 7. Pressure contours in the heat exchanger equipped with different vortex generators: (a) Sample 1, (b) Sample 2 and (c) Sample 3.

The variations of the hydraulic-thermal performance as a function of Re in the heat exchanger equipped with different vortex generators and various φ are shown in figure 8. As observed, in all cases, the values of the PEC are greater than unity. This indicates that the use of the vortex generator in any geometric configuration in the present study is appropriate in terms of the PEC index. A decreasing trend with increasing Re and nanofluid φ is observed. Sample 3 exhibits the highest PEC.

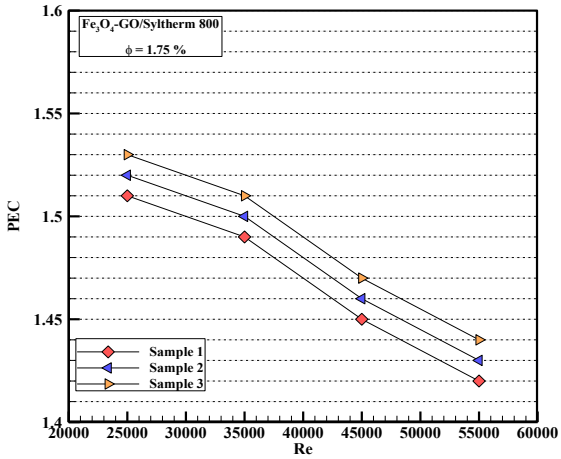

(a)

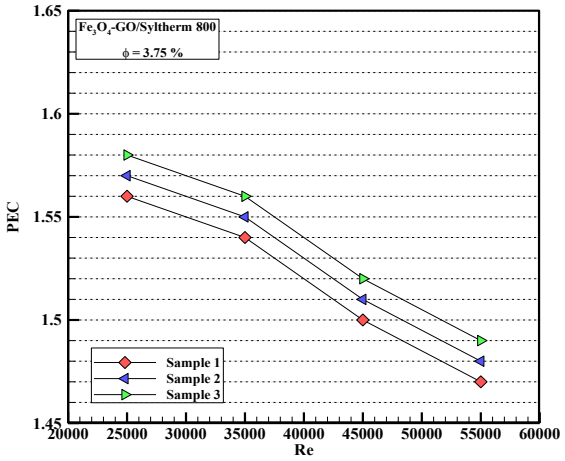

(b)

Fig. 8. Variations of the PEC as a function of the Re in the heat exchanger equipped with different vortex generators and (a) φ of 1.75%, and (b) φ of 3.75%.

PEC variations versus Re, similar to the previous figure, are presented in figure 9 for the case with an imposed magnetic field. The same trends are also found in this figure. The important point is an increase in the PEC by imposing a magnetic field of up to 20%. Furthermore, the more magnetic field, the higher the PEC.

These results indicate that despite the increased pressure drop, there is a positive trade-off between heat transfer and energy consumption. This finding is particularly important for systems that require high heat transfer but have pumping cost limitations, such as HVAC systems or water desalination plants.

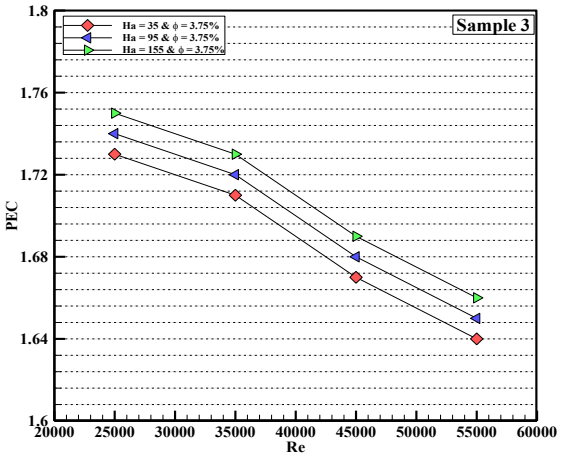

Fig. 9. Variations of the PEC as a function of the Re in the heat exchanger equipped with Sample 3 vortex generators and φ of 3.75%.

Figure 10 shows the turbulent kinetic energy contours in the heat exchanger equipped with different vortex generators. From the obtained results, it can be stated that the maximum value of turbulent kinetic energy occurs in the heat exchanger equipped with the sample 3 vortex generator. This leads to higher mixing and improves heat transfer.

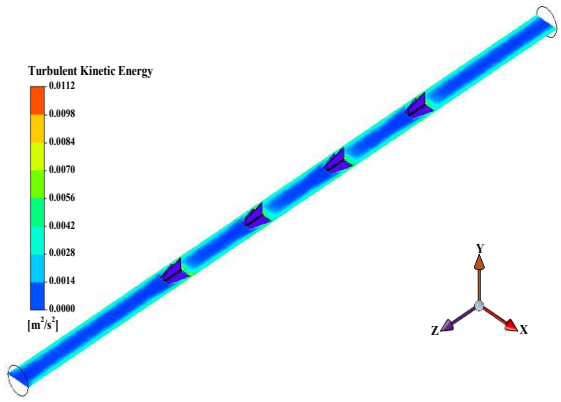

(a)

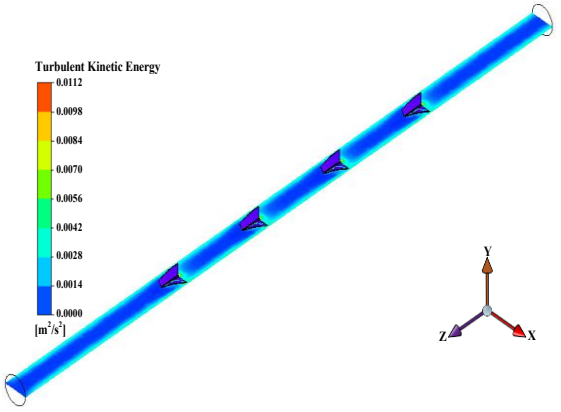

(b)

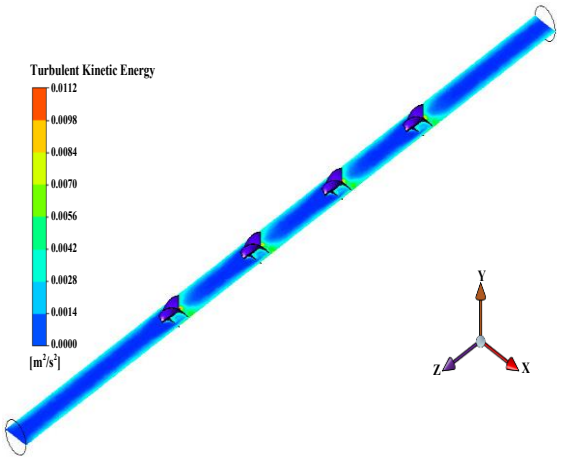

(c)

Fig. 10. Turbulent kinetic energy contours in the heat exchanger equipped with different vortex generators: (a) Sample 1, (b) Sample 2 and (c) Sample 3.

4.3. Exergy Analysis

The variations of exergy efficiency are shown in figure 11 for three types of vortex generators. As observed, exergy efficiency exhibits an upward trend with increasing Re and nanoparticle φ. However, an increase in the twist ratio of the vortex generator blades leads to a decrease in exergy efficiency in the double-tube heat exchanger.

Using sample 1 and a φ of 3.75%, the exergy efficiency increases by 25.43% as Re rises from 25,000 to 55,000. However, using Sample 2 and a φ of 3.75%, the exergy efficiency increases by 25.81%. This value for Sample 3 is 26.50%.

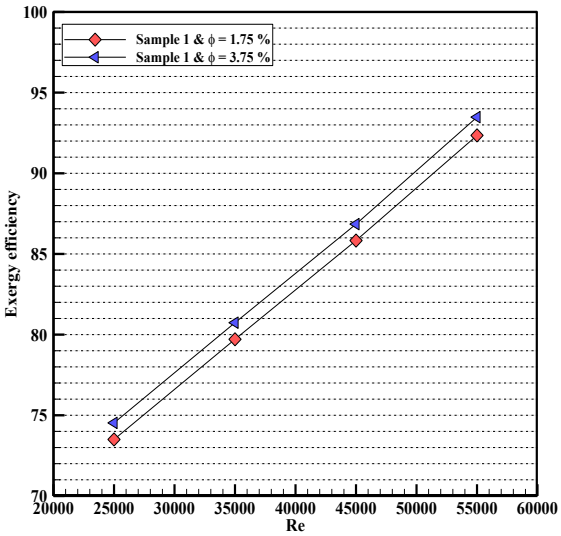

(a)

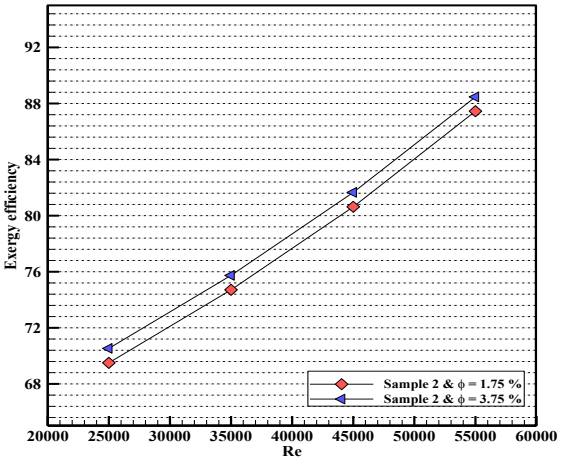

(b)

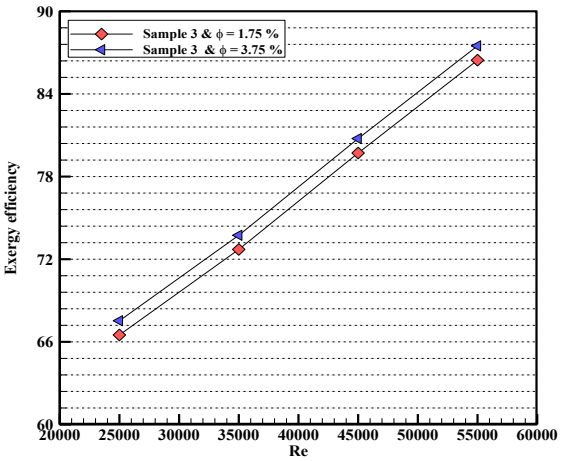

(c)

Fig. 11. Variations of the exergy efficiency as a function of the Re in the heat exchanger equipped with different vortex generators and (a) φ of 0, (b) φ of 1.75%, and (c) φ of 3.75%.

The variations of exergy efficiency by applying the sample 3 vortex generator under the influence of a magnetic field at a φ of 3.75% are shown in figure 12. As observed, with an increase in the Hartmann number from 35 to 155, the exergy efficiency increases. Additionally, as Re increases to 35,000, the exergy efficiency rises and then decreases. It can be concluded that the use of a magnetic field achieves maximum exergy efficiency at Re=35,000 and a Hartmann number of 155 when using Sample 3.

These findings help to identify the optimal operating point of the system. For example, in the design of a heat exchanger for a solar power plant, setting Re≈35,000 and Ha=155 can maximize energy efficiency and minimize exergy destruction.

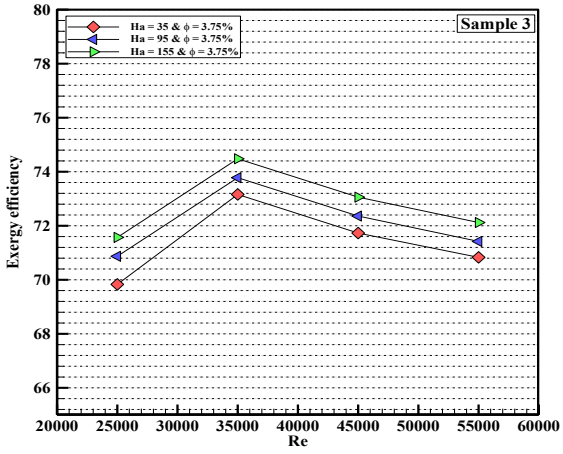

Fig. 12. Variations of the exergy efficiency as a function of the Re in the heat exchanger equipped with Sample 3 vortex generators and φ of 3.75%.

5. Conclusions

In this study, the simultaneous effect of a magnetic field, hybrid nanofluid, and vortex generators with novel geometries on the hydro-thermal performance of a double-tube heat exchanger was comprehensively investigated. The results showed that the combination of these technologies leads to a significant improvement in heat transfer, exergy efficiency, and the Performance Evaluation Criterion (PEC). The most important findings are as follows:

- Heat Transfer Enhancement: The use of vortex generator sample 3 at a volume concentration of 3.75% hybrid nanofluid and a Reynolds number of 55,000 resulted in a 60.18% increase in the Nusselt number (Nu) compared to the case without a turbulence promoter. This improvement is due to the creation of intense mixing and a reduction in the thermal boundary layer.
- Influence of Magnetic Field: Applying a magnetic field with a Hartmann number of 155 increased the exergy efficiency by up to 26.50%. This improvement is due to the control of the movement of iron oxide nanoparticles and reducing irreversible energy losses.
- Optimization of PEC: sample 3, under a strong magnetic field (Ha=155), showed the highest PEC (20% improvement), indicating a desirable balance between heat transfer and pressure drop. This result is a significant step in the design of energy-efficient, high-performance heat exchangers.
- Non-linear Behavior of Exergy Efficiency: Exergy efficiency increased up to Re=35,000, but decreased thereafter due to increased frictional losses. This finding confirms the need for precise adjustment of operating parameters to achieve the optimal point.

These results are applicable in industries such as power plants, air conditioning systems, and chemical processes that require efficient heat transfer. The use of a magnetic field as a control tool enables the dynamic management of heat exchanger performance.

The present study is based on numerical simulations; it is suggested that experimental tests be carried out for more accurate validation. Investigating the effects of corrosion and the long-term stability of the hybrid nanofluid under operating conditions is recommended. The use of advanced turbulence models (such as LES) and multi-objective optimization with artificial intelligence algorithms can improve the accuracy of predictions. This research provides a novel framework for integrating heat transfer enhancement technologies and paves the way for the development of sustainable energy systems in the future.

Funding Statement

This research did not receive any specific grant from funding agencies in the public, commercial, or not-for-profit sectors.

Conflicts of Interest

The author declares that there is no conflict of interest regarding the publication of this article.

Authors Contribution Statement

Alireza Aghaei: Conceptualization; Formal Analysis; Software; Project administration; Supervision; Writing – Review & Editing.

Alireza Mirzaei: Investigation; Software Validation; Visualization; Methodology; Roles/Writing – Original Draft.

Abolfazl Fattahi: Writing – Review.

References

[1] Bayat, J. Nikseresht, A.H., 2012. Thermal performance and pressure drop analysis of nanofluids in turbulent forced convective flows. *International Journal of Thermal Sciences*, 60, pp. 236-243.

[2] Bhuiya, M.M.K., Chowdhury, M.S.U., Shahabuddin, M., Saha, M., Memon, L.A., 2013. Thermal characteristics in a heat exchanger tube fitted with triple twisted

tape inserts. *International Communications in Heat and Mass Transfer,* 48, pp. 124-132.

[3] Dnyaneshwar, R, Waghole., R.M., Warkhedkar., V.S., Kulkarni., R.K., Shrivastva., 2014. Experimental Investigations on Heat Transfer and Friction Factor of Silver Nanofliud in Absorber/Receiver of Parabolic Trough Collector with Twisted Tape Inserts. *Energy Procedia*, 45, pp. 558-567.

[4] Smith, E.A., Chayut, N., Pongjet, P., 2013. Effect of Twin Delta-Winged Twisted-Tape on Thermal Performance of Heat Exchanger Tube. *Heat Transfer Engineering*, 34(15).

[5] Kim, S.K., Ha, M.Y., Son, C. et al, 2014. An experimental study on the pressure drop and heat transfer through straight and curved small diameter tubes. *J. Mech. Sci. Technol.*, 28, pp. 797–809.

[6] Hamdi, E.A., Ahmed, M.I., Yusoff, M.Z., 2015. Heat transfer enhancement in a triangular duct using compound nanofluids and turbulators. *Applied Thermal Engineering*, 91, pp. 191-201.

[7] Zhang, J., Diao, Y., Zhao, Y., Zhang, Y., 2017. An experimental investigation of heat transfer enhancement in minichannel: Combination of nanofluid and micro fin structure techniques. *Experimental Thermal and Fluid Science*, 81, pp. 21-32.

[8] Mashoofi, N., Pesteei, S.M., Moosavi, A., Sadighi Dizaji, H., 2017. Fabrication method and thermal-frictional behavior of a tube-in-tube helically coiled heat exchanger which contains turbulator. *Applied Thermal Engineering*, 111, pp. 1008-1015.

[9] Sheikholeslami, M., Ganji, D.D., Gorji-Bandpy, M., 2016. Experimental and numerical analysis for effects of using conical ring on turbulent flow and heat transfer in a double pipe air to water heat exchanger. *Applied Thermal Engineering*, 100, pp. 805-819.

[10] Shirvan, K.M., Mamourian, M., Mirzakhanlari, S., Ellahi, R., 2017. Numerical investigation of heat exchanger effectiveness in a double pipe heat exchanger filled with nanofluid: A sensitivity analysis by response surface methodology. *Powder Technology*, 313, pp. 99-111.

[11] Panahi, D., Zamzamian, K., 2017. Heat transfer enhancement of shell-and-coiled tube heat exchanger utilizing helical wire turbulator. *Applied Thermal Engineering*, 115, pp. 607-615

[12] Bezaatpour, M., Goharkhah, M., 2019. Convective heat transfer enhancement in a double pipe mini heat exchanger by magnetic field induced swirling flow. *Applied Thermal Engineering*, 110, pp. 380-410.

[13] Sheikholeslami, M., Haq, R.U., Shafee, A., Li, Z., 2019. Heat transfer behavior of nanoparticle enhanced PCM solidification through an enclosure with V shaped fins. *International Journal of Heat and Mass Transfer*, 130, pp.1322–1342.

[14] Qi, C., Tang, J., Ding, Z., Yan, Y., Guo, L., Ma, Y., 2019. Effects of rotation angle and metal foam on natural convection of nanofluids in a cavity under an adjustable magnetic field. *International Communications in Heat and Mass Transfer,* 109, 104349.

[15] Abdelrazek, A.H., Kazi, S.N., Alawi, O.A., Yusoff, N., Oon, C.S. and Ali, H.M., 2020. Heat transfer and pressure drop investigation through pipe with different shapes using different types of nanofluids. *Journal of Thermal Analysis and Calorimetry*, 139(3), pp.1637-1653.

[16] Berberovi´c, E., and Biki´c, S., 2019. Computational Study of Flow and Heat Transfer Characteristics of EG-Si3N4 Nanofluid in Laminar Flow in a Pipe in Forced Convection Regime. In *the 1st International Conference on Nanofluids (ICNf) and 2nd European Symposium on Nanofluids (ESNf)*, 26–28 June 2019, Castelló, Spain. Conference Proceedings. pp. 226–230.

[17] Bahiraei, M., Mazaheri, N., Sheykh Mohammadi, M., Moayedi, H., 2019. Thermal performance of a new nanofluid containing biologically functionalized graphene nanoplatelets inside tubes equipped with rotating coaxial double-twisted tapes. *International Communications in Heat and Mass Transfer*, 108, 104305.

[18] Hajialigol, N., Daghigh, R., 2020. The evaluation of the first and second laws of thermodynamics for the pulsating MHD nanofluid flow using CFD and machine learning approach. *Journal of the Taiwan Institute of Chemical Engineers, 150, pp. 84-93*.

[19] Zhou, J., Alizadeh, A., Ashraf Ali, M., Sharma, K., 2023. The use of machine learning in optimizing the height of triangular obstacles in the mixed convection flow of two-phase MHD nanofluids inside a rectangular cavity. *Engineering Analysis with Boundary Elements,* 150, pp. 84-93.

[20] Bhaskar, K., Sharma, K. & Bhaskar, K. 2023. Cross-diffusion and chemical reaction effects of a MHD nanofluid flow inside a divergent/convergent channel with heat source/sink. *J. Therm. Anal. Calorim.,* 148, pp. 573–588.

[21] Tavakoli, M., Soufivand, MR., 2023. Investigation of entropy generation, PEC, and efficiency of parabolic solar collector containing water/Al2O3− MWCNT hybrid nanofluid in the presence of finned and perforated twisted tape turbulators using a two-phase flow scheme. *Engineering Analysis with Boundary Elements*, 148, pp. 324-335.

[22] El-Shafay, AS., Mohamed, AM., Ağbulut Ü, 2023. Gad MS. Investigation of the effect of magnetic field on the PEC and exergy of heat exchanger filled with two-phase hybrid nanofluid, equipped with an edged twisted tape. *Engineering Analysis with Boundary Elements,* 148, pp. 153-164.

[23] Mohadjer, A., Nobakhti, M.H., Nezamabadi, A., Ajarostaghi, SS., 2024. Thermohydraulic analysis of nanofluid flow in tubular heat exchangers with multi-blade turbulators: The adverse effects. *Heliyon,* 10(9), 72, pp. 436-461

[24] Wang, L., Wang, J., Tang, J., Zho, X., 2024. Enhancing heat exchanger efficiency with novel perforated cone-shaped turbulators and nanofluids: a computational study. *Chemical Product and Process Modeling*, 19(1), pp. 147-158.

[25] Sheikholeslami, M., Abd Ali, F.A., 2024. Influence of vortex generator on performance of concentrated solar photovoltaic module in existence of heat sink. *Applied Thermal Engineering,* 253, 123758.

[26] Hejazian, M., Moraveji, M.K., Beheshti, A., 2014. Comparative study of Euler and mixture models for turbulent flow of Al2O3 nanofluid inside a horizontal tube. *International Communications in Heat and Mass Transfer*, 52, pp. 152-158.

[27] Aminfar, H., Mohammadpourfard, M., Mohseni, F., 2012. Two-phase mixture model simulation of the hydro-thermal behavior of an electrically conductive ferrofluid in the presence of magnetic fields. *Journal of Magnetism and Magnetic Materials*, 324, pp. 830-842.

[28] Xiong, Q., Jafaryar, M., Divsalar, A., Sheikholeslami, M., Shafee, A., Vo, D.D., Khan, M.H., Tlili, I. and Li, Z., 2019. Macroscopic simulation of nanofluid turbulent flow due to compound turbulator in a pipe. *Chemical Physics*, 527, p.110475.

[29] Amer Qureshi, M., Hussain, S., Adil Sadiq, M., 2021. Numerical simulations of MHD mixed convection of hybrid nanofluid flow in a horizontal channel with cavity: Impact on heat transfer and hydrodynamic forces. *Case Studies in Thermal Engineering*, 27, p. 101323.

[30] Typical Properties of SYLTHERM 800 Fluid 1. n.d.

[31] Nasirzadehroshenin, F., Maddah, H., Sakhaeinia, H., Pourmozafari, A., 2019. Investigation of exergy of double-pipe heat exchanger using synthesized hybrid nanofluid developed by modeling. *International Journal of Thermophysics*, 40, pp. 1-24.

[32] Sundar L.S., K.Singh, M., Antonio M.C.F., Sousa, C.M., 2017. Experimental investigation of the thermal transport properties of graphene oxide/Co3O4 hybrid nanofluids. *International Communications in Heat and Mass Transfer*, 84, pp. 1-10.

[33] Sheikholeslami, M., Shehzad, S.A., 2018. Numerical analysis of Fe3O4–H2O nanofluid flow in permeable media under the effect of external magnetic source. *International Journal of Heat and Mass Transfer*, 118, pp. 182-192.

[34] Ma, Y., Mohebbi, R., Rashidi, M.M., Yang, Z., 2019. MHD convective heat transfer of Ag-MgO/water hybrid nanofluid in a channel with active heaters and coolers. *International Journal of Heat and Mass Transfer*, 137, pp. 714-726.

[35] Al-Asadi, M.T., Alkasmoul, F.S., Wilson, M.C., 2016. Heat transfer enhancement in a micro-channel cooling system using cylindrical vortex generators. *International Communications in Heat and Mass Transfer*, 74, pp.40-47.

[36] Bellos, E., Tzivanidis, C., Tsimpoukis, D., 2018. Optimum number of internal fins in parabolic trough collectors. *Applied Thermal Engineering*, 137, pp. 669-677.

[37] Yang, J., Feng, Z., 2024. Assessing the use of PEC and jf methods for strengthening the evaluation of new heat exchangers. *Heliyon*, 10(10), pp. 142-169.

[38] Gürdal, M., Pazarlıoğlu, H.K., Tekir, M., Arslan, K., Gedik, E., 2022. Numerical investigation on turbulent flow and heat transfer characteristics of ferro-nanofluid flowing in dimpled tube under magnetic field effect. *Applied Thermal Engineering*, 200, 117655.